

# Localization and functional characterization of the alternative oxidase in *Naegleria*

Diego Cantoni<sup>1</sup>  | Ashley Osborne<sup>1</sup>  | Najwa Taib<sup>2,3</sup> | Gary Thompson<sup>4</sup> | Rubén Martín-Escolano<sup>1</sup>  | Eleanna Kazana<sup>1</sup> | Elizabeth Edrich<sup>5</sup> | Ian R. Brown<sup>6</sup> | Simonetta Gribaldo<sup>2</sup>  | Campbell W. Gourlay<sup>5</sup>  | Anastasios D. Tsaousis<sup>1</sup> 

<sup>1</sup>Laboratory of Molecular & Evolutionary Parasitology, RAPID Group, School of Biosciences, University of Kent, Canterbury, UK

<sup>2</sup>Unit Evolutionary Biology of the Microbial Cell, Department of Microbiology, Institut Pasteur, UMR CNRS 2001, Paris, France

<sup>3</sup>Hub Bioinformatics and Biostatistics, Department of Computational Biology, Institut Pasteur, USR 3756 CNRS, Paris, France

<sup>4</sup>NMR Facility, School of Biosciences, University of Kent, Canterbury, UK

<sup>5</sup>Kent Fungal Group, RAPID Group, School of Biosciences, University of Kent, Canterbury, UK

<sup>6</sup>Bioimaging Facility, School of Biosciences, University of Kent, Canterbury, UK

## Correspondence

Anastasios D. Tsaousis, RAPID Group, School of Biosciences, University of Kent, Canterbury, Kent CT2 7NJ, UK.  
Emails: [A.Tsaousis@kent.ac.uk](mailto:A.Tsaousis@kent.ac.uk) and [tsaousis.anastasios@gmail.com](mailto:tsaousis.anastasios@gmail.com)

## Funding information

Alfonso Martín Escudero Foundation; Gordon and Betty Moore Foundation; Biotechnology and Biological Sciences Research Council, Grant/Award Number: BB/M009971/1

## Abstract

The alternative oxidase (AOX) is a protein involved in supporting enzymatic reactions of the Krebs cycle in instances when the canonical (cytochrome-mediated) respiratory chain has been inhibited, while allowing for the maintenance of cell growth and necessary metabolic processes for survival. Among eukaryotes, alternative oxidases have dispersed distribution and are found in plants, fungi, and protists, including *Naegleria* ssp. *Naegleria* species are free-living unicellular amoeboflagellates and include the pathogenic species of *N. fowleri*, the so-called “brain-eating amoeba.” Using a multidisciplinary approach, we aimed to understand the evolution, localization, and function of AOX and the role that plays in *Naegleria*'s biology. Our analyses suggest that AOX was present in last common ancestor of the genus and structure prediction showed that all functional residues are also present in *Naegleria* species. Using cellular and biochemical techniques, we also functionally characterize *N. gruberi*'s AOX in its mitochondria, and we demonstrate that its inactivation affects its proliferation. Consequently, we discuss the benefits of the presence of this protein in *Naegleria* species, along with its potential pathogenicity role in *N. fowleri*. We predict that our findings will spearhead new explorations to understand the cell biology, metabolism, and evolution of *Naegleria* and other free-living relatives.

## KEYWORDS

adaptation, confocal microscopy, evolution, mitochondria, *Naegleria*, respiration

Diego Cantoni and Ashley Osborne contributed equally.

This is an open access article under the terms of the [Creative Commons Attribution](https://creativecommons.org/licenses/by/4.0/) License, which permits use, distribution and reproduction in any medium, provided the original work is properly cited.

© 2022 The Authors. *Journal of Eukaryotic Microbiology* published by Wiley Periodicals LLC on behalf of International Society of Protistologists.

*NAEGLERIA gruberi* is a free-living, heterotrophic, microbial eukaryote, and a close relative of *N. fowleri*, the so-called “brain-eating amoeba”. It is a nonpathogenic member of the excavate supergroup, which contains key pathogens such as Kinetoplastids (*Trypanosoma*, *Leishmania*), *Giardia* and *Trichomonas*, and is evolutionarily distant from animals, fungi, and plants (Adl et al., 2019). *Naegleria* resides primarily as an amoebic (trophozoite) form, but upon environmental stimuli can transform into a flagellate, synthesizing basal bodies and flagella de novo, or encyst to allow for dispersion (De Jonckheere et al., 2001). It possesses all the major organelles deemed to be canonical for eukaryotes, including nucleus, mitochondria, peroxisomes (Fritz-Laylin et al., 2010), and a Golgi (Herman et al., 2018). This cellular complexity is reflected in the *N. gruberi* genome sequence (Fritz-Laylin et al., 2010) found to encode an extensive complement of cellular machinery and was argued to be reflective of the ancient sophistication present in the last eukaryotic common ancestor (Koonin, 2010).

Found in soils and freshwater worldwide, *N. gruberi* can thrive in a wide range of osmotic and oxygenic conditions (De Jonckheere, 1979; De Jonckheere, 2014; Týmł et al., 2016). It has the capacity for full aerobic and anaerobic metabolism, and was predicted to have assimilated unique biochemical adaptations both within and outside the mitochondria (Fritz-Laylin et al., 2010, 2011; Ginger et al., 2010). Among those, only a handful of pathways have been localized and characterized, in the trophozoite stage of this microbial eukaryote. Some examples include the cytosolic localization and functional characterization of the [FeFe]-hydrogenase (Tsaousis et al., 2014), the mitochondrial localization and functional characterization of ferritin (Mach et al., 2018), and the oxygen-dependent metabolism of lipids (Bexkens et al., 2018). While the last report provided a hint on the function of *Naegleria*'s alternative oxidase (AOX), a thorough investigation on this important oxygen-dependent enzyme is lacking.

The alternative oxidase (AOX) is a terminal oxidase typically involved in bypassing the electron transport chain in plant mitochondria, even though it has also been identified and localized in the mitochondria and related organelles of many nonrelated microbial eukaryotes including trypanosomes (Clarkson et al., 1989), *Candida albicans* (Yan et al., 2009), *Cryptosporidium* (Roberts et al., 2004), and *Blastocystis* (Stechmann et al., 2008; Tsaousis et al., 2018). Due to its absence in humans, the protein is considered a potential drug target and has been well studied in some of these pathogenic species (Duvenage et al., 2019; Shiba et al., 2013; Tsaousis et al., 2018). Despite the wide distribution and extensive research on this group of proteins, their overall physiological roles are still unclear (Moore & Albury, 2008). Intriguingly, it has been suggested that AOX may be involved in maintaining tricarboxylic acid cycle turnover under high cytosolic phosphorylation potential, stress

tolerance (oxygen), and thermogenesis (Finnegan et al., 2004; Moore et al., 2013).

Herein, we employed a multiphasic approach to characterize the AOX of *N. gruberi*, while comparing it with both the *N. fowleri* and the *N. lovaniensis* homologues and examining their origins. Upon structural characterization of all the counterparts, we generated a specific polyclonal antibody against *N. gruberi* AOX, with which we localized the protein in *N. gruberi*'s mitochondria using a combination of assorted cellular approaches. Experiments with high-resolution respirometry demonstrated that the *N. gruberi* homologue confers cyanide resistance, as previously described (Bexkens et al., 2018). Based on this and the previously published data, this study represents a comprehensive characterization of AOX in *Naegleria* species, which could provide further understanding into the biochemical adaptations of this peculiar and highly adaptable microbial eukaryote.

## MATERIALS AND METHODS

### Bioinformatic analysis

The predicted amino acid sequences of the alternative oxidase homologues of *N. fowleri* and *N. lovaniensis* were obtained from Genbank (NCBI) using the following accession numbers; GCA\_008403515.1 (*N. fowleri*) and GCA\_003324165.1 (*N. lovaniensis*). The amino acid sequence of the AOX from *N. gruberi* was obtained from uniprot (D2V4B2). The Phyre2 Web portal for protein modeling, prediction, and analysis was used in intensive mode (Kelley et al., 2015) to derive the structure for NgAOX. Structures were then downloaded and analyzed using PyMol. For sequence alignment Clustal Omega (Sievers et al., 2011) was used, output was downloaded as fasta file and analyzed using Jalview 2.11.0 (Waterhouse et al., 2009). Sequence identifiers for AOX alignments were as follows: *Trypanosoma brucei brucei* (Q26710), *Cryptosporidium parvum* (Q6W3R4), yeast; *Candida albicans* (A0A1D8PEM4), plant; *Arabidopsis thaliana* (Q39219), and, fungi; *Neurospora crassa* (Q01355).

### Phylogenetic analysis

Three local databanks of proteomes, representative of all diversity from eukaryotes, bacteria, and proteobacteria were assembled from the National Center for Biotechnology Information (NCBI): 193 proteomes from Eukaryotes (one per genus); 1017 proteomes from Bacteria (3 per family), and 1082 proteomes from Proteobacteria (1 per genus). Homology searches were performed using HMMSEARCH, from the HMMER-3.1b2 package (Johnson et al., 2010), with the option—cut\_ga to screen all the proteomes in the three databanks for the presence of AOX pfam

domain (PF01786.17). All the hits were then manually curated to discard false positives. The remaining hits were aligned using MAFFT-v7.407 (Katoh & Standley, 2013) with the linsi option and trimmed with BMGE-1.1 (Criscuolo & Gribaldo, 2010) using the BLOSUM30 substitution matrix to select unambiguously aligned positions. A maximum likelihood tree was then generated using IQTREE-1.6.12 (Nguyen et al., 2015) under the TEST option with 1000 ultrafast bootstrap replicates.

## Cell culture

*Naegleria gruberi* strain NEG-M (kindly provided by Lillian Fritz-Laylin, Biology Department, University of Massachusetts, Amherst, USA) was cultured in M7 media at 28°C (Tsaousis et al., 2014) or PYNFH at 25°C (Bexkens et al., 2018). Cells were passaged every 3–5 days to prevent overconfluency.

## Antibody generation

A 16 amino acids peptide (nh2- CMHRDYNHDMS-DKHRA –conh2) was designed by Eurogentec based on the provide sequence of AOX of *Naegleria gruberi* (XP\_002672918) (see Figure S2). A total of 5 mg of the peptide was coupled with the carrier protein KHL (Keyhole Limpet Hemocyanin) and was subsequently used to inoculate a rabbit (through the Eurogentec's speedy program) for antibody production. The antibody's affinity (Eurogentec; Peptide: 1911009, Rabbit 237) was confirmed through ELISA.

## Cell fractionation and western blots

To separate organelles from cytosol, cell fractionation by centrifugation was carried out as previously described (Herman et al., 2018). Lysates were mixed with 4× sample buffer and heated to 95°C for 10 min. Samples were then loaded in two tris-glycine gels for gel electrophoresis. One gel was subjected to Coomassie staining overnight and destained the following day to assess equal loading. The other gel was transferred to PVDF membrane using a trans-blot turbo transfer system according to the manufacturer's protocol (Bio-rad). Membranes were blocked with 5% milk in TBS buffer containing 0.5% tween-20 for 1 h at room temperature. Primary antibody staining was carried out overnight at 4°C with the following antibody dilutions: anti-AOX 1:1000, and previously published antibodies anti-HydE 1:1000 and, SdhB 1:1000 (Tsaousis et al., 2014). Membranes were washed four times with TBS-T for 5 min prior to secondary staining with HRP-conjugated goat anti-mouse and goat

anti-rabbit antibodies (Invitrogen). For detection, membranes were incubated with ECL reagent (Bio-rad) for 30 s and imaged using syngene G:BOX imager. Membranes were stripped with mild stripping buffer composed of 13 mM glycine, 3.5 mM sodium dodecyl sulfate, 1% tween-20, pH 2.2. PVDF membranes were washed twice for 10 min in mild stripping buffer, followed by two washes in PBS for 5 min, and lastly two washes for 5 min with TBS-T, prior to blocking for the next immunoprobe.

## Immunofluorescence microscopy

*Naegleria gruberi* was seeded onto sterile poly-L-lysine treated glass coverslips in a 6-well plate and incubated overnight at 25°C. The following day, the cells were treated with 250 nM MitoTracker Red for 30 min. The media was then aspirated, and cells were washed with 1× PBS, followed by fixation using 2% formaldehyde for 20 min. After fixation, 2% formaldehyde was removed and cells were permeabilized with 0.1% triton-X 100 for 10 min. After permeabilization, cells were washed three times with 1× PBS and blocked using 3% bovine serum albumin in PBS for 1 h. Primary antibody staining was carried out at room temperature for 1 h with custom-made AOX antibodies (Eurogentec; Peptide: 1911009, Rabbit 237), diluted to 1:1000. Secondary antibody staining was carried out for 1 h in the dark using anti-Rabbit-IgG-Alexa 488. Slides were washed and mounted using Prolong Gold Antifade with DAPI. Laser Confocal Microscopy was carried out using the LSM 880 Laser Confocal with Airyscan by Zeiss. Laser sets used were 405, 488, and 594, with airyscan detector plate imaging for high resolution. Images were captured and analyzed using Zen software suite by Zeiss.

## Immunoelectron microscopy

Samples were prepared as previously described (Herman et al., 2018). Blocking of the samples was achieved via a 1-h incubation in 2% BSA in PBS with TBST (20 mM Tris, 0.1% BSA, 500 mM NaCl and 0.05% Tween 20, pH7.4). Grids were washed in TBST between block and primary. Primary antibody staining was performed by incubating AOX antibodies at 1:10, 1:50, and 1:100 dilutions overnight at 4°C. The sample grids were then incubated for 30 min at room temperature, with the corresponding gold-conjugated secondary antibodies. Counter-staining was achieved by incubation with 4.5% Uranyl acetate in 1% acetic acid in PBS for 15 min and a 2-min incubation in Reynold's lead citrate. The sample grids were imaged with a Jeol 1230 Transmission Electron Microscope operated at 80 kV and images were captured with a Gatan One view digital camera.

## High-resolution respirometry

Real-time respirometry was monitored using an OROBOROS Oxygraph-2k with Clark polarographic oxygen electrodes and automatic titration-injection micropump. The chambers of the oxygraph were calibrated using 2 ml of either M7 or PYNFH media without glucose for 20 min. *N. gruberi* cells were seeded in the chamber at a density of 100,000 cells per ml. Respiration was monitored before and during drug additions. The drugs used to assess respiration were added in the following order: 1 mM potassium cyanide, 5  $\mu$ M antimycin A, and 1.5 mM salicylhydroxamic acid (SHAM). The experiment was then repeated with the drug additions in reverse order. Student's *t*-test was used to determine significance.

## Cell proliferation assay

*Naegleria* cells were seeded at a density of 2000 cells per well of a clear F-bottom 96-well plate and incubated in identical conditions as stated above. The plate was placed on a Juli™ Stage live cell monitoring system, programmed to capture an image of each well every hour for 5 days. On day-2, wells were inoculated with concentrations of SHAM at 1, 0.1, 0.001 and 0.001 mM. Plates were then incubated for a further 3 days. At the end of the experiment, the images were used to count cell numbers using ImageJ. Using an image with a scale bar, we used the grid function with a known area per square that was applied to all images taken at 0, 24, 48, 72, 96, and 120 h. Using the cell counter function, we counted the number of cells in a grid square and multiplied it to the surface area size of a F-bottom 96-well plate to estimate the total cell number per well. The experiment was completed with three biological replicates, whereby each biological replicate consisted of three technical replicates. Cell counts were graphed using GraphPad Prism 8.

## RESULTS

### Phylogenetic analysis of alternative oxidase proteins

We carried out an exhaustive search for AOX homologs in updated eukaryotic and bacterial databanks. As bacterial hits were mainly from proteobacteria, we also searched for AOX homologs in a proteobacteria databank with more diversity within this phylum. We identified 323 AOX homologs: 265 from 193 eukaryotic taxa, 56 from 1,082 proteobacterial taxa, and 2 from 896 bacterial taxa (other than proteobacteria) (Table S1).

Regarding the eukaryotic distribution, in addition to previously described groups Alveolata, Euglenozoa,

Metazoa, Choanoflagellates, Stramenopiles, Fungi, Rhodophyta, Heterolobosea, and Viridiplantae (Pennisi et al., 2016), we identified AOX homologs in some eukaryotes that were not reported: Apusozoa, Amoebozoa, Filasterea, Haptophyceae, and Rhizaria. No homologs were found in Kipferlia, Metamonada, and Hexamitida (Figure S1 and Table S1). Bacterial hits were much less diversified, as they are restricted to alphaproteobacteria, betaproteobacteria, and gammaproteobacteria. The other two hits belong to Bacteroidetes and the CPR (Candidate Phyla Radiation) and they probably correspond to transfers from proteobacterial taxa (Figure S1). Our phylogenetic analysis shows that AOX homologs of Metazoans (UFB = 86%), Haptophyceae, Choanoflagellata (UFB = 100%), and Heterolobosea (UFB = 100%; inset Figure 1) form distinct and monophyletic groups pointing toward the presence of an AOX in the ancestors of each group. Regarding bacterial sequences, although they branch together and form a monophyletic clade (UFB = 97%), it seems that proteobacterial taxa transferred AOX sequences to other bacteria (Bacteroidetes and CPR) and to some Euglenozoa. This bacterial clade forms a sister group of Streptophyta and Rhodophyta (UFB = 97%); however, it is not clear which eukaryotic group transferred AOX sequences to proteobacteria.

The presence of the two separate and monophyletic groups Streptophyta (UFB = 100%), Chlorophyta (UFB = 82%) shows that, although the presence of AOX could not be inferred in the ancestor of Archaeplastida, it can be inferred in the ancestors of both groups. Finally, regarding Fungi, the presence of three separate and monophyletic groups containing Ascomycota and Basidiomycota (UFB = 80%), Chytridiomycota (UFB = 100%) and a mix of Zoopagomycota, Chytridiomycota, Cryptomycota, Mucoromycota, Blastocladiomycota, and Microsporidia (UFB = 74%), suggests that AOX was acquired at least three times independently in this group.

### Amino acid alignments reveal conserved residues in *Naegleria gruberi*, *Naegleria fowleri* and *Naegleria lovaniensis*

The amino acid sequences of AOX in *N. gruberi*, *N. fowleri*, and *N. lovaniensis* were aligned against the AOX found in protists; *Trypanosoma brucei brucei*, *Cryptosporidium parvum*, yeast; *Candida albicans*, plant; *Arabidopsis thaliana* and, fungus; *Neurospora crassa*. The N-termini displayed little conservation. However, key conserved residues were detected across all species from the middle of the sequences, continuing toward the C-terminus (Figure S2). Most of the conserved residues localized in the alpha helical arms, including the residues responsible for membrane interaction, diiron binding domain and, three universally conserved tyrosines (Table S2). The presence of these key features strongly

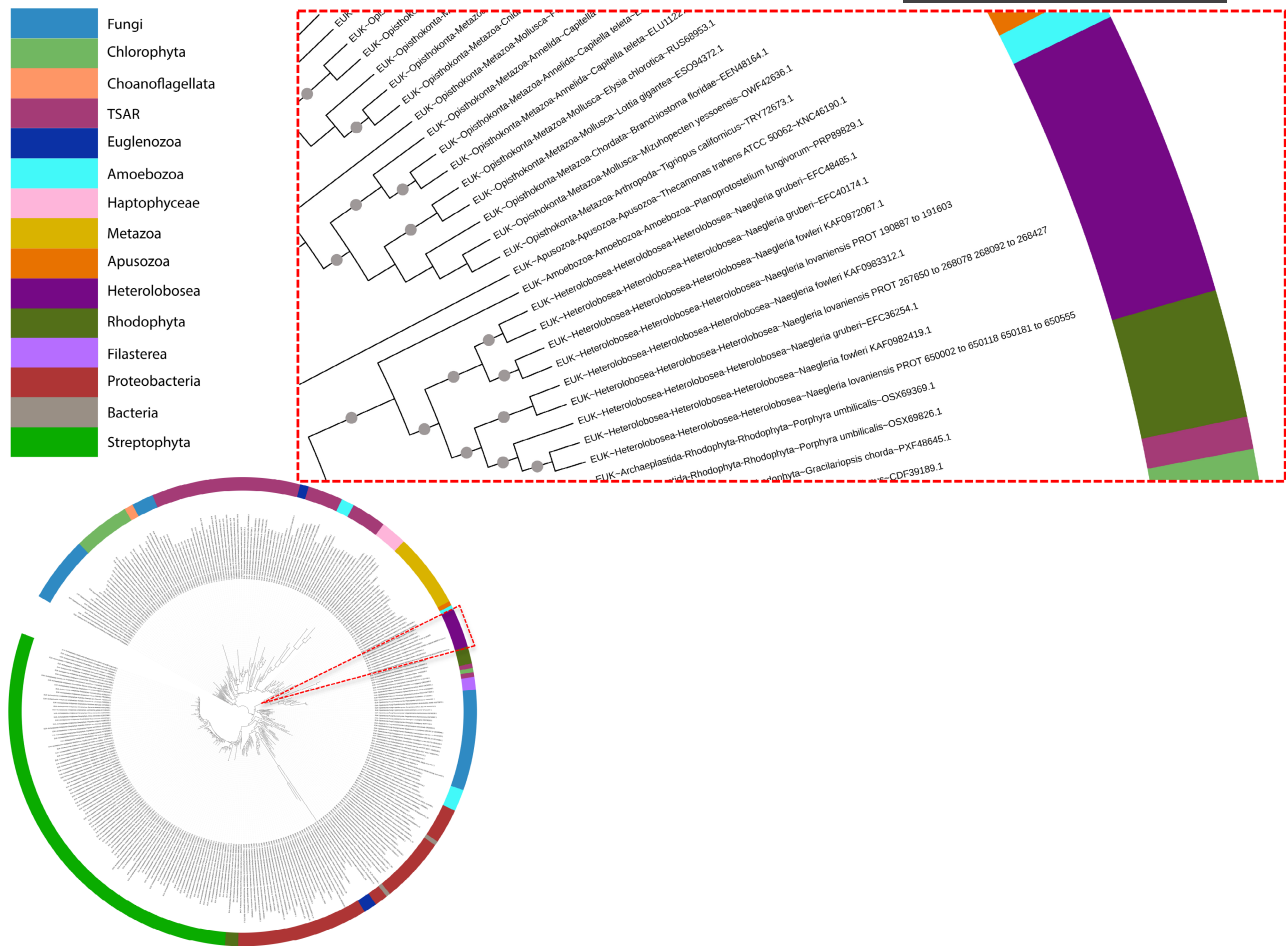


**FIGURE 1** Phylogenetic trees demonstrating the origin of alternative oxidases in heterolobosea. Maximum likelihood tree of AOX homologs in eukaryotes and bacteria (323 sequences, 148 amino acid positions). The tree was inferred with IQTREE using the LG + I + G4 model selected under the BIC criterion. Gray dots correspond to supports higher than 80%. The scale bar corresponds to the average number of substitutions per site. Inset focus on the heterolobosean section of the tree, demonstrating the evolution and duplications events through the *Naegleria* genus. Full phylogenetic tree can be found in Figure S1

suggests that *Naegleria*'s predicted AOX would retain functional activity.

### Structure modeling of AOX from *Naegleria gruberi*

Using Phyre2, we were able to generate models of the NgAOX monomer. The resulting model reveals a monomer containing the characteristic four-bundle helix, in which resides the active site (Figure 2). The active site is composed of the characteristic four glutamate residues and two histidine residues which are responsible for diiron binding. In addition, the universally conserved tyrosine residue necessary for activity is present at residue number 175. Furthermore, helices  $\alpha 1$  and  $\alpha 4$  contains a strong hydrophobic region, also a key feature of AOX, as these helices are involved in membrane insertion. Amino acid conservation of glycine 85 and glycine 165 between all *Naegleria* species and *Trypanosoma* contribute to the structural kink of both  $\alpha 2$  and  $\alpha 5$  helices.

We also observed conservation between amino acids responsible for membrane-binding regions and for dimerization (Table S2). These amino acid conservations highlight the conserved structure of AOX, its characteristic helices and hydrophobicity patch for membrane anchoring.

### Localization of AOX in *Naegleria gruberi*

To verify the presence and localization of AOX, fractionation by centrifugation was carried out to isolate the mitochondria and cytosol. Using a custom-made antibody raised against *N. gruberi* AOX, our Western blot analysis reveals the presence of AOX in the mitochondrial fraction and not in the cytosolic fraction (Figure 3C) Successful fractionation was confirmed by immunoblotting Hydrogenase E protein, which localizes exclusively in the cytosol and succinate dehydrogenase, a previously confirmed mitochondrial marker (Tsaousis et al., 2014). The localization of AOX was also carried out by

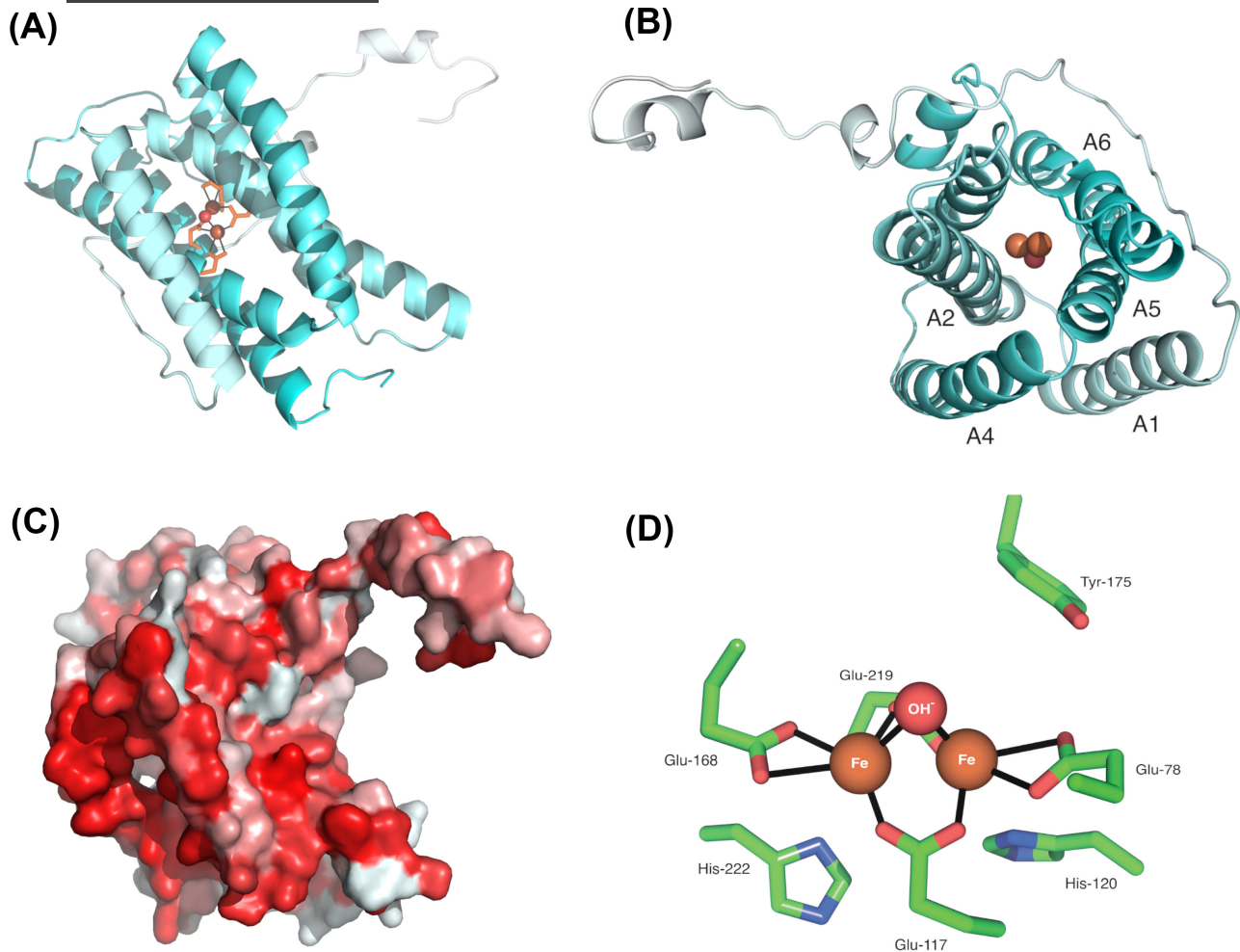


**FIGURE 2** Structural modeling of *Naegleria gruberi* AOX reveals canonical features. Using Phyre2 we modeled the structure of ngAOX. We observed the presence of the di-iron domain and alpha-helical bundles, as viewed from the side (A) and top-down (B). Rendering the structure by hydrophobicity shows the typical hydrophobic patch required for membrane anchoring (C). Close up view of the di-iron domain model derived by Phyre2 (D)

immunofluorescent microscopy, whereby *N. gruberi* cells were stained with mitotracker red before fixation, and subsequently fixed and immunostained for detecting AOX. Our imaging reveals a high degree of colocalization between the mitotracker signal and the AOX signal derived from the secondary antibodies. This indicates that AOX is localized in the mitochondria (Figure 3A,B and Figure S3). To further confirm these observations, we have subsequently carried out immunoelectron microscopy (IEM) on resin fixed *N. gruberi* sample grids. As a result, we detected positive signal inside derived from the immunogold labeling, strongly suggesting its localization is within the inner membrane of the mitochondria (Figure 4).

### Real-time respirometry reveals AOX confers cyanide resistance

To assess whether *N. gruberi* respire from either the classical respiratory chain or through AOX, real-time respirometry data were collected. Cells were cultured

for three days and washed with either M7 or PYNFH media without the addition of glucose. Afterward, 2 ml of cell resuspension was seeded into the respirometer chambers at a density of  $10^5$  cells per ml. After establishing the routine respiration, a series of drugs were added sequentially to each chamber and oxygen flux was monitored (Figure 5). Initially, 1 mM of complex IV inhibitor potassium cyanide was injected into the chambers, revealing an increase in oxygen flux and decrease in oxygen concentration, which would suggest that respiration via alternative oxidase pathway is active. The addition of complex III inhibitor, Antimycin A, had no effect on respiration. Lastly, addition of 1.5 mM of AOX inhibitor SHAM resulted in a significant decrease in respiration (Figure 5A,B). When the experiment was repeated with drug additions in the reverse order, the SHAM treatment resulted in a significant decrease in respiration, whereas Antimycin A and KCN had no further effects on respiration (Figure 5C,D). This would suggest that *N. gruberi* respire predominantly via the AOX pathway under the conditions used.

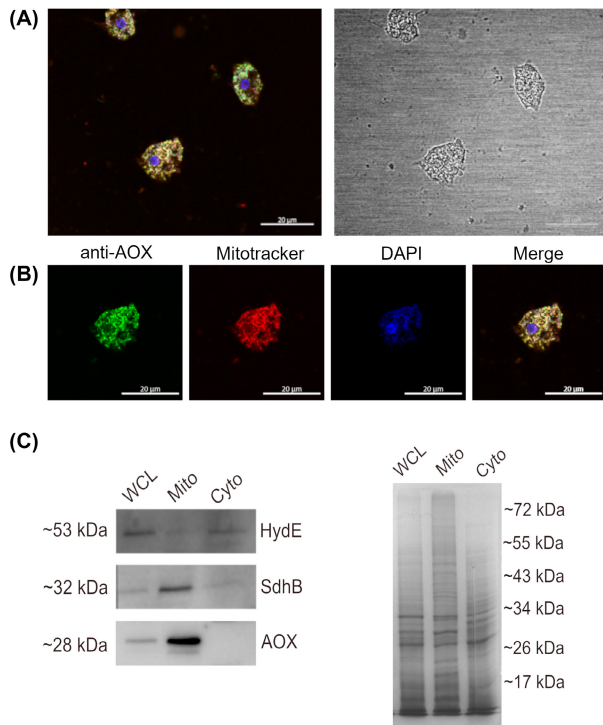


**FIGURE 3** Confocal microscopy and western blot reveal mitochondrial localization of AOX. (A and B) *Naegleria gruberi* cells were treated with mitotracker red prior to fixation and then probed with AOX antibodies (green). Nuclear marker and mtDNA staining is shown in blue (DAPI staining). Our confocal imaging reveals a high degree of colocalization between the mitotracker red signal and the green signal derived from immunoprobable AOX. These results provide visual confirmation of the expression of AOX and their localization in the mitochondria. Localization figures of more *N. gruberi* cells can be found in Figure S3. For western blotting lysates were fractionated by centrifugation to yield samples containing pelleted mitochondrial fraction and a clarified cytosolic fraction. Successful fractionation from the whole cell lysate was confirmed by immunoblotting (left-hand side) for hydrogenase maturase E (HydE) that localizes in the cytosol, and succinate dehydrogenase B (SdhB), which localizes exclusively in the mitochondria (C). Immunostaining against AOX revealed a band around ~28 kDa in the whole cell lysate and mitochondrial fraction only. A coomassie stain was carried out to the parallel SDS-PAGE gel parallel to assess equal loading between samples (right-hand side)

### The presence of SHAM in culture media reduces cellular proliferation

Due to the decrease respiration in *N. gruberi* in the presence of SHAM, we opted to evaluate cell growth under varying concentrations of SHAM using a Juli™ Stage live cell monitoring system (Figure 6). Cells were grown in 96-well culture plates for 48 h to allow proliferation. At the 48-hour mark, we pipetted varying amounts of SHAM in culture media to reach the following final concentrations; 1, 0.1, 0.01, and 0.001 mM. The plate was then returned to the incubator for another 72 h. By counting the number of cells under each condition, we were able to verify the negative effect of SHAM on proliferation. Concentrations of SHAM at 1–0.1 mM were effective at

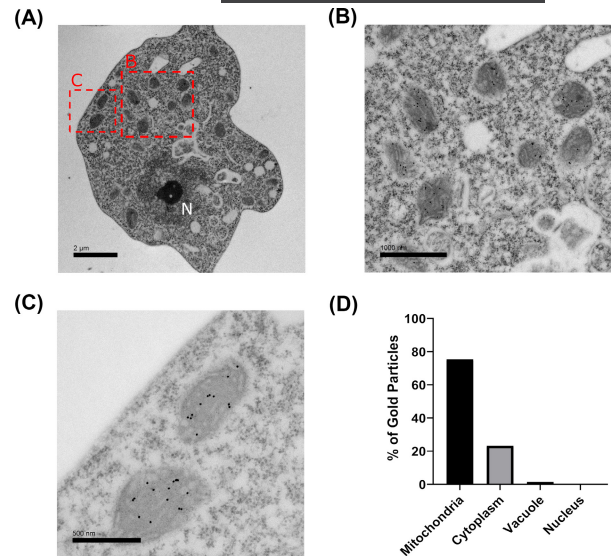


**FIGURE 4** Immunoelectron microscopy reveals AOX localization within the inner mitochondrial membrane. Fixed *Naegleria gruberi* samples were probed for IEM to assess their localization in the mitochondria (A). The AOX signal derived by the immunogold secondary antibodies bound against AOX primary antibodies localizes predominantly inside the mitochondria (B, C). The gold particles were then quantified based on their localisation (D).

stopping cell proliferation altogether, whereas 0.01 mM SHAM greatly reduced cell proliferation. SHAM concentration of 0.001 mM had no effect on cell proliferation, as the cell counts followed a similar pattern to the negative control.

## DISCUSSION

The genome of *Naegleria gruberi* (Fritz-Laylin et al., 2010) encodes several homologues of alternative oxidases, but until now, there was no thorough report to investigate the origin and distribution of these proteins within microbial eukaryotes. Our sophisticated search and analyses suggest that the AOX gene was present in the ancestors of multiple eukaryotic groups, suggesting potential acquisition at earlier stages in the eukaryotic evolution. Specifically, for the *Naegleria* species, our phylogenetic analysis indicates that AOX gene duplication took place prior to speciation events, which further suggests the earlier requirement of two homologues as an adaptation to the unique lifestyles of these organisms. In *N. gruberi*, these homologues have been previously shown to be differentially expressed during the organism's two major stages, trophozoite and flagellate (<https://phycocosm.jgi.doe.gov/pages/blast-query.jsf?db=Naegr1>) (Fritz-Laylin et al., 2010). The reason behind this is currently unknown, and no conclusions can be extracted from the primary amino acid sequences of the two homologues. Our sequence alignment analysis reveals that the key residues required for AOX to be functional are present

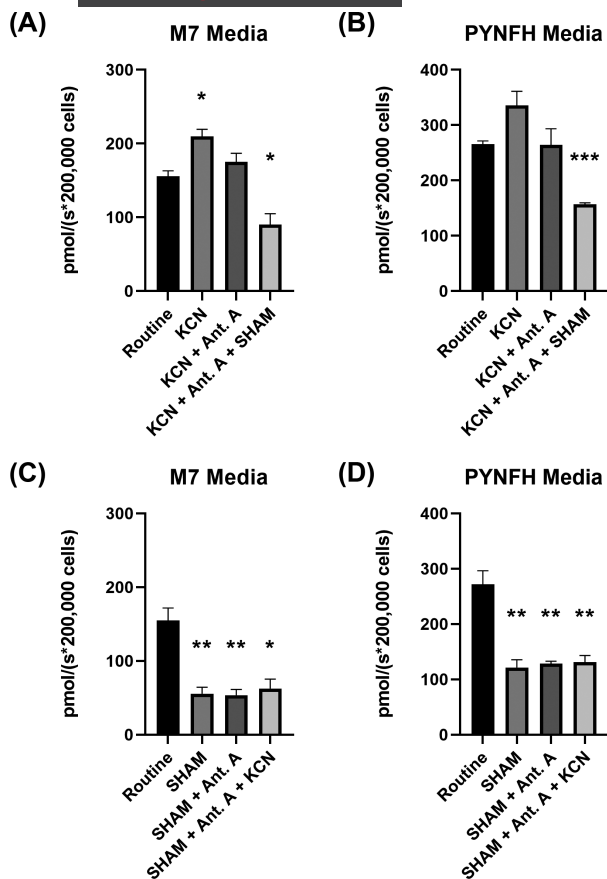


**FIGURE 5** High resolution real-time respirometry reveals cyanide resistant respiration. *Naegleria gruberi* cells were subjected to real-time respirometry in the presence of metabolic inhibitors to assess respiration using either M7 (A, C) or PYNFH (B, D) culture media without glucose. Cells were added to the chambers without the presence of inhibitors to assess normal respiration, followed by the addition of a mitochondrial complex inhibitor. The order of inhibitors was KCN (complex IV inhibitor) followed by Antimycin A (complex III inhibitor) and SHAM (AOX inhibitor) (A, B). The experiments were then completed in reverse order (C, D). KCN did not display decreases in respiration, whereas SHAM significantly reduced respiration. Results consist of three independent biological repetitions. Student's *t* tests were carried out between each drug condition to the routine respiration. *p* values; \* $<0.05$ , \*\* $<0.01$  \*\*\* $<0.001$

across all homologues and all three *Naegleria* species. One of the key domains presented in the sequences is the diiron domain, characterized by four glutamic acid residues and two histidine residues involved in forming hydrogen bonds with  $\text{Fe}^{2+}$  and  $\text{Fe}^{1+}$  ions, of which the latter are considered to be universally conserved (Moore et al., 2013). In addition, our sequence alignment reveals the presence of the three universally conserved tyrosine residues (Moore et al., 2013) in the electron transport chain (Moore et al., 2013; Shiba et al., 2013). Interestingly, our sequence alignment revealed a deviation in conservation of the residue trp-151 (*TbAOX*), including between the pathogenic *N. fowleri*, nonpathogenic *N. lovaniensis* and *N. gruberi* species. It has previously been reported that a mutation from trp-206 (trp-151 on *tbaOX*) to ala-206

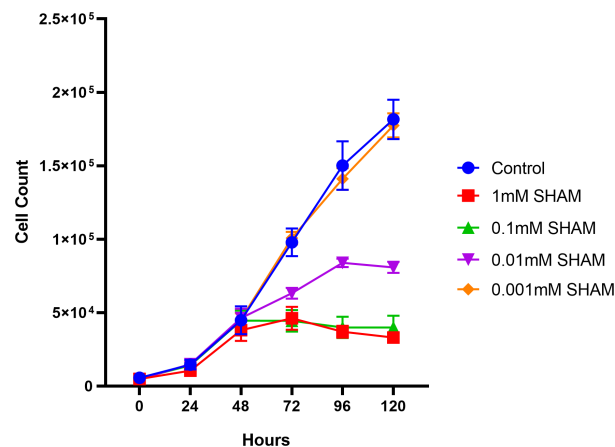


**FIGURE 6** Growth of *Naegleria gruberi* is reduced in increasing concentrations of SHAM. Using the JuLI™ Stage Live cell monitoring system, we were able to monitor the growth rates of *N. gruberi* cells in varying concentrations of SHAM. Cells were seeded in wells of a 96-well plate and left to grow for 48 h prior to the addition of SHAM at 1, 0.1, 0.01 and 0.001 mM concentration. By counting cells, we noticed a significant decrease in cell numbers when challenged with 1 and 0.1 mM SHAM. In the presence of 0.01 mM SHAM we saw a decrease in proliferation rate, peaking at 96 h. We observed no effect using SHAM at 0.001 mM. Error bars are standard error of the mean

resulted in a decrease in respiration of 95% (Crichton et al., 2010). However, wet laboratory experiments would be required to ascertain the effect of the difference in respiration found in *Naegleria* species.

Following up from the in silico analysis, we aimed to biochemically characterize the *N. gruberi* AOX homolog. It had been previously experimentally demonstrated that *N. gruberi*'s preferred food substrate are lipids over glucose, which was subsequently associated with the unique abundance of metabolites in the brain (Bexkens et al., 2018). The authors demonstrated that *N. gruberi* has a biochemically active AOX, but they did not show any localization. We have designed a peptide and generated an anti-*Naegleria* polyclonal antibody that could cross-react with all *Naegleria* species and be used for localization studies. Our immunoblotting results show a strong band appearing at 28 kDa, which was the predicted mass of *N. gruberi*'s AOX. This signal only appeared in the whole cell lysate and mitochondrial fraction, with no signal in the cytosolic fraction. This data were strengthened by our immunofluorescent microscopy experiments, which revealed a high degree of colocalization between the AOX staining and a commercial mitochondrial stain (Tsaousis et al., 2014). Lastly, an experiment using immunogold labeling showed staining signal from inside the mitochondria, which we find encouraging as AOX is located on the inner mitochondrial membrane (Berthold et al., 2000).

Next, real-time respirometry data showed strong evidence of AOX being an active component in *N. gruberi* as the addition of KCN did not lower the oxygen flux. Remarkably, we did observe significant differences

between the two culture media used, which could be explained due to the effect of the media in the growth conditions and potentially metabolism of this protist (Zaongo, et al., 2018). Interestingly, previous work explored the potential cyanide resistance of *N. gruberi* as part of a larger metabolomic study (Bexkens et al., 2018). The authors reported an 80% decrease in respiration, which contrasts with our results. The authors also reported that addition of SHAM further decreased respiration by 14%. The differences between the results reported here and the aforementioned study is likely to be attributed to the differing growth conditions or prolonged differential adaptations of the laboratory strains (Schuster, 2002). Unexpectedly, there was a high residual respiration after the addition of the inhibitor, which could be due to the presence of other nonmitochondrial oxidases, or to the presence of proto-globin and hemerythrin, which have been recently shown to interact with oxygen in vitro in *N. gruberi* (Malych et al., 2022). Nonetheless, our cellular and biochemical data confirm their hypothesis regarding the presence of AOX in *N. gruberi* mitochondria. This, however, leads to significant questions in the pursuit of elucidating the complex metabolic mechanisms in *N. gruberi*, in particular, which environmental conditions favor expression and utilization of AOX, there is no report demonstrating the endurance of *Naegleria* species under, for example, hypoxic conditions. *Naegleria* species favor warm and moist environments and have been isolated from lakes, rivers, geothermal springs along with man-made bodies of water such as swimming pools, thermal effluent, sewage sludge and water-cooling circuits from power station [for review, see (Chalmers, 2014)]. As a result, *Naegleria* species seem to acclimatize in various temperatures, turbidities, and metal concentrations, which subsequently affect the mitochondrial functions. In other organisms, mainly plants, AOX has been implicated in metabolic and signaling homeostasis and was demonstrated to be particularly important during a variety of stresses, including alterations in temperature, nutrient deficiency, oxygen levels and metal toxicity (Saha et al., 2016; Vanlerberghe, 2013). Such observations may be true for *Naegleria* as well, and further investigations using these different parameters are required to understand the true role of the various AOX homologs in *Naegleria*'s survival. For example, a previous report has shown differences between metabolic activities of iron-saturated and iron-restricted trophozoites of *N. gruberi*, which could subsequently be attributed to potential iron homeostasis centrally regulated by the mitochondria (Mach et al., 2018). Again, it will be interesting to further investigate the role and function of the AOX in such mechanisms.

While reviewing the adaptations of *Naegleria* in the various environments, we cannot avoid discussing the potential role of AOX in the pathogenesis of *N. fowleri*. A recently published omics approach investigating the potential genes that could be driving the pathogenicity of *N. fowleri* demonstrated up-regulation of mitochondrial

energy conversion genes including those involved in ubiquinone biosynthesis, isocitrate dehydrogenase (TCA cycle), complex I and complex III of oxidative phosphorylation (Herman et al., 2021). While the authors have demonstrated up-regulation of enzymes indirectly involved in oxidative stress pathway (e.g., agmatine deiminase), they were not able to demonstrate any significant change in the expression levels of any of the *N. fowleri* AOX homologs (Herman et al., 2021). Based on these observations, it would be interesting to investigate the expression levels of AOX from the amoebas collected directly from the brain, either through transcriptomics and/or proteomics, as well as investigate whether this protein is essential for the survival of *N. fowleri* in such a complicated and variable environment.

It has been observed that there are significant differences in concentration levels of metabolites between various brain regions (Cichočka & Bereš, 2018). *N. fowleri* is typically found in olfactory bulb of the brain (Moseman, 2020), which it has a unique metabolic network signature and is highly abundant in various salts (e.g., sodium, potassium, and calcium), metals (e.g., iron, copper, and magnesium) (Gardner et al., 2017), metabolites (histidine-containing dipeptides such as anserine, carnosine, b-alanine), cholesterol, poly-unsaturated fatty acids and prostaglandins (Choi et al., 2018), as well as featuring variable concentrations of oxygen (Özugur et al., 2020). Differences in the concentrations of these factors have been previously shown to provide stimuli for alterations in the expression of AOX in plants (Vanlerberghe, 2013) and trypanosomes (Vassella et al., 2004). As previously discussed, AOX was also shown to be implicated in metabolic and signaling homeostasis and was demonstrated to be particularly important during a variety of stresses, including alterations in temperature, nutrient deficiency, oxygen levels and metal toxicity (Saha et al., 2016). Additionally, it has been demonstrated that salt stress negatively impacts mitochondria function, resulting in decreased electron transport activities, with increased mitochondrial ROS and lipid peroxidation, followed by subsequent induction of mitochondrial ROS-scavenging systems, including increase activity of AOX (Ferreira et al., 2008; Mhadhbi et al., 2013; Saha et al., 2016). We speculate that similar implications could be associated with the function of AOX in *N. fowleri* populating the brain. Demonstrating that anti-AOX drugs are effective against *Naegleria* growth, is of great importance to investigate whether these proteins are essential for the survival of *N. fowleri* in the brain, and determine if it is possible to efficiently utilize these compounds (Barsottini et al., 2020; Ebiloma et al., 2019; Murphy & Lang-Unnasch, 1999) against the “brain-eating amoeba.”

Herein, we provide the first thorough investigation of the localization and functional characterization of the alternative oxidase proteins in *Naegleria* species.

These single-protein-focused studies are essential in contributing to our understanding of the biochemical and cellular adaptations of this exceptional microbial eukaryote as well as provide another piece in *Naegleria*'s evolutionary puzzle. As a result, our investigation on the function of the AOX provides an additional step toward developing this organism as a model to understand various pan-eukaryotic adaptations and more importantly how metabolism could affect its opportunistic nature.

## ACKNOWLEDGMENTS

This research was supported by BBSRC research grant (BB/M009971/1) to ADT. EK was supported by a Betty and Gordon Moore Foundation grant to ADT. R.M.E. was supported by the Alfonso Martín Escudero Foundation.

## AUTHORS' CONTRIBUTIONS

D.C., A.O., S.G., C.W.G., and A.D.T. designed the experiments. D.C., A.O., N.T., R.M.E., E.K., I.R.B., and E.E. conducted the experiments. D.C., N.T. and G.T. performed the data analysis. D.C. and A.D.T. wrote the manuscript and all co-authors reviewed and approved it.

## ORCID

Diego Cantoni  <https://orcid.org/0000-0001-8527-7719>

Ashley Osborne  <https://orcid.org/0000-0002-2804-8298>

Rubén Martín-Escolano  <https://orcid.org/0000-0002-6262-9344>

Simonetta Gribaldo  <https://orcid.org/0000-0002-7662-021X>

Campbell W. Gourlay  <https://orcid.org/0000-0002-2373-6788>

Anastasios D. Tsaousis  <https://orcid.org/0000-0002-5424-1905>

## REFERENCES

- Adl, S.M., Bass, D., Lane, C.E., Lukeš, J., Schoch, C.L., Smirnov, A. et al. (2019) Revisions to the classification, nomenclature, and diversity of eukaryotes. *Journal of Eukaryotic Microbiology*, 66(1), 4–119. Available from: <https://doi.org/10.1111/jeu.12691>
- Barsottini, M.R.O., Copsey, A., Young, L., Baroni, R.M., Cordeiro, A.T., Pereira, G.A.G. et al. (2020) Biochemical characterization and inhibition of the alternative oxidase enzyme from the fungal phytopathogen *monilophthora perniciosa*. *Communications Biology*, 3, 263. Available from: <https://www.nature.com/articles/s42003-020-0981-6>
- Berthold, D.A., Andersson, M.E. & Nordlund, P. (2000) New insight into the structure and function of the alternative oxidase. *Biochimica Et Biophysica Acta – Bioenergetics*, 1460(2–3), 241–254. Available from: [https://doi.org/10.1016/S0005-2728\(00\)00149-3](https://doi.org/10.1016/S0005-2728(00)00149-3)
- Bexkens, M.L., Zimorski, V., Sarink, M.J., Wienk, H., Brouwers, J.F., De Jonckheere, J.F. et al. (2018) Lipids are the preferred substrate of the protist *Naegleria gruberi*, relative of a human brain pathogen. *Cell Reports*, 25(3), 537–543.e3. Available from: <https://doi.org/10.1016/j.celrep.2018.09.055>
- Chalmers, R.M. (2014) Chapter twenty – *Naegleria*. In: Percival, S.L., Yates, M.V., Williams, D.W., Chalmers, R.M. & Gray, N.F. (Eds.) *Microbiology of waterborne diseases*, 2nd Edition. London: Academic Press, pp. 407–416. Available from: <https://doi.org/10.1016/B978-0-12-415846-7.00020-2>
- Choi, W.T., Tosun, M., Jeong, H.H., Karakas, C., Semerci, F., Liu, Z. et al. (2018) Metabolomics of mammalian brain reveals regional differences. *BMC Systems Biology*, 12(S8). Available from: <https://doi.org/10.1186/s12918-018-0644-0>
- Cichocka, M. & Bereś, A. (2018) From fetus to older age: a review of brain metabolic changes across the lifespan. *Ageing Research Reviews*, 46, 60–73. Available from: <https://doi.org/10.1016/j.arr.2018.05.005>
- Clarkson, A.B., Bienen, E.J., Pollakis, G. & Grady, R.W. (1989) Respiration of bloodstream forms of the parasite *Trypanosoma brucei brucei* is dependent on a plant-like alternative oxidase. *Journal of Biological Chemistry*, 264(30), 17770–17776.
- Crichton, P.G., Albury, M.S., Affourtit, C. & Moore, A.L. (2010) Mutagenesis of the *Sauromatum guttatum* alternative oxidase reveals features important for oxygen binding and catalysis. *Biochimica Et Biophysica Acta – Bioenergetics*, 1797(6–7), 732–737. Available from: <https://doi.org/10.1016/j.bbabi.2009.12.010>
- Crisuolo, A. & Gribaldo, S. (2010) BMGE (block mapping and gathering with entropy): a new software for selection of phylogenetic informative regions from multiple sequence alignments. *BMC Evolutionary Biology*, 10(1), 210. Available from: <https://doi.org/10.1186/1471-2148-10-210>
- De Jonckheere, J.F. (1979) Occurrence of *Naegleria* and *Acanthamoeba* in aquaria. *Applied and Environmental Microbiology*, 38(4), 590–593. Available from: <https://doi.org/10.1128/aem.38.4.590-593.1979>
- Duvenage, L., Munro, C.A. & Gourlay, C.W. (2019) The potential of respiration inhibition as a new approach to combat human fungal pathogens. *Current Genetics*, 65(6), 1347–1353. Available from: <https://doi.org/10.1007/s00294-019-01001-w>
- Ebiloma, G.U., Balogun, E.O., Cueto-Díaz, E.J., de Koning, H.P. & Dardonville, C. (2019) Alternative oxidase inhibitors: mitochondrion-targeting as a strategy for new drugs against pathogenic parasites and fungi. *Medicinal Research Reviews*, 39(5), 1553–1602. Available from: <https://doi.org/10.1002/med.21560>
- Ferreira, A.L., Arrabaça, J.D., Vaz-Pinto, V. & Lima-Costa, M.E. (2008) Induction of alternative oxidase chain under salt stress conditions. *Biologia Plantarum*, 52(1), 66–71. Available from: <https://doi.org/10.1007/s10535-008-0009-4>
- Finnegan, P.M., Soole, K.L. & Umbach, A.L. (2004) *Alternative mitochondrial electron transport proteins in higher plants*. Springer, pp. 164–217. Available from: [https://doi.org/10.1007/978-1-4020-2400-9\\_9](https://doi.org/10.1007/978-1-4020-2400-9_9)
- Fritz-Laylin, L.K., Ginger, M.L., Walsh, C., Dawson, S.C. & Fulton, C. (2011) The *Naegleria* genome: a free-living microbial eukaryote lends unique insights into core eukaryotic cell biology. *Research in Microbiology*, 162(6), 607–618. Available from: <https://doi.org/10.1016/j.resmic.2011.03.003>
- Fritz-Laylin, L.K., Prochnik, S.E., Ginger, M.L., Dacks, J.B., Carpenter, M.L., Field, M.C. et al. (2010) The genome of *Naegleria gruberi* illuminates early eukaryotic versatility. *Cell*, 140(5), 631–642. Available from: <https://doi.org/10.1016/j.cell.2010.01.032>
- Gardner, B., Dieriks, B.V., Cameron, S., Mendis, L.H.S., Turner, C., Faull, R.L.M. et al. (2017) Metal concentrations and distributions in the human olfactory bulb in Parkinson's disease. *Scientific Reports*, 7(1). Available from: <https://doi.org/10.1038/s41598-017-10659-6>
- Ginger, M.L., Fritz-Laylin, L.K., Fulton, C., Zacheus Cande, W. & Dawson, S.C. (2010) Intermediary metabolism in protists: a sequence-based view of facultative anaerobic metabolism in evolutionarily diverse eukaryotes. *Protist*, 161(5), 642–671. Available from: <https://doi.org/10.1016/j.protis.2010.09.001>

- Herman, E.K., Greninger, A., van der Giezen, M., Ginger, M.L., Ramirez-Macias, I., Miller, H.C. et al. (2021) Genomics and transcriptomics yields a system-level view of the biology of the pathogen *Naegleria fowleri*. *BMC Biology*, 19(1), 142. Available from: <https://doi.org/10.1186/s12915-021-01078-1>
- Herman, E.K., Yiangou, L., Cantoni, D.M., Miller, C.N., Marciano-Cabral, F., Anthonyrajah, E. et al. (2018) Identification and characterisation of a cryptic Golgi complex in *Naegleria gruberi*. *Journal of Cell Science*. Available from: <https://doi.org/10.1242/jcs.213306>
- Johnson, L.S., Eddy, S.R. & Portugaly, E. (2010) Hidden Markov model speed heuristic and iterative HMM search procedure. *BMC Bioinformatics*, 11(1). Available from: <https://doi.org/10.1186/1471-2105-11-431>
- Jonckheere, J.F.D. (2014) What do we know by now about the genus *Naegleria*? *Experimental Parasitology*, 145, S2–S9. Available from: <https://doi.org/10.1016/j.exppara.2014.07.011>
- Jonckheere, J.F., De, S., Brown, P.J., Dobson, B.S.R. & Pernin, P. (2001) The amoeba-to-flagellate transformation test is not reliable for the diagnosis of the genus *Naegleria*. Description of three new *Naegleria* spp. *Protist*, 152(2), 115–121. Available from: <https://doi.org/10.1078/1434-4610-00049>
- Katoh, K. & Standley, D.M. (2013) MAFFT multiple sequence alignment software version 7: improvements in performance and usability. *Molecular Biology and Evolution*, 30(4), 772–780. Available from: <https://doi.org/10.1093/molbev/mst010>
- Kelley, L.A., Mezulis, S., Yates, C.M., Wass, M.N. & Sternberg, M.J.E. (2015) The Phyre2 web portal for protein modeling, prediction and analysis. *Nature Protocols*, 10(6), 845–858. Available from: <https://doi.org/10.1038/nprot.2015.053>
- Koonin, E.V. (2010) The incredible expanding ancestor of eukaryotes. *Cell*, 140(5), 606–608. Available from: <https://doi.org/10.1016/j.cell.2010.02.022>
- Mach, J., Bíla, J., Ženíšková, K., Arbon, D., Malych, R., Glavanaková, M. et al. (2018) Iron economy in *Naegleria gruberi* reflects its metabolic flexibility. *International Journal for Parasitology*, 48(9–10), 719–727. Available from: <https://doi.org/10.1016/j.ijpara.2018.03.005>
- Malych, R., Füssy, Z., Ženíšková, K., Arbon, D., Hampl, V., Hrdý, I. et al. (2022) The response of *Naegleria gruberi* to oxidative stress. *Metallomics*, mfac009. Available from: <https://doi.org/10.1093/mtomcs/mfac009>
- Mhadhbi, H., Fotopoulos, V., Mylona, P.V., Jebara, M., Elarbi Aouani, M. & Polidoros, A.N. (2013) Alternative oxidase 1 (Aox1) gene expression in roots of *Medicago truncatula* is a genotype-specific component of salt stress tolerance. *Journal of Plant Physiology*, 170(1), 111–114. Available from: <https://doi.org/10.1016/j.jplph.2012.08.017>
- Moore, A.L. & Albury, M.S. (2008) Further insights into the structure of the alternative oxidase: from plants to parasites. *Biochemical Society Transactions*, 36(5), 1022–1026. Available from: <https://doi.org/10.1042/BST0361022>
- Moore, A.L., Shiba, T., Young, L., Harada, S., Kita, K. & Ito, K. (2013) Unraveling the heater: new insights into the structure of the alternative oxidase. *Annual Review of Plant Biology*, 64(1), 637–663. Available from: <https://doi.org/10.1146/annurev-arplant-042811-105432>
- Moseman, E.A. (2020) Battling brain-eating amoeba: enigmas surrounding immunity to *Naegleria fowleri*. *PLoS Path*, 16(4), e1008406. Available from: <https://doi.org/10.1371/journal.ppat.1008406>
- Murphy, A.D. & Lang-Unnasch, N. (1999) Alternative oxidase inhibitors potentiate the activity of atovaquone against *Plasmodium falciparum*. *Antimicrobial Agents and Chemotherapy*. Available from: <https://doi.org/10.1128/aac.43.3.651>
- Nguyen, L.T., Schmidt, H.A., Von Haeseler, A. & Minh, B.Q. (2015) IQ-TREE: a fast and effective stochastic algorithm for estimating maximum-likelihood phylogenies. *Molecular Biology and Evolution*, 32(1), 268–274. Available from: <https://doi.org/10.1093/molbev/msu300>
- Özuger, S., Kunz, L. & Straka, H. (2020) Relationship between oxygen consumption and neuronal activity in a defined neural circuit. *BMC Biology*, 18(1). Available from: <https://doi.org/10.1186/s12915-020-00811-6>
- Pennisi, R., Salvi, D., Brandi, V., Angelini, R., Ascenzi, P. & Polticelli, F. (2016) Molecular evolution of alternative oxidase proteins: a phylogenetic and structure modeling approach. *Journal of Molecular Evolution*, 82(4–5), 207–218. Available from: <https://doi.org/10.1007/s00239-016-9738-8>
- Roberts, C.W., Roberts, F., Henriquez, F.L., Akiyoshi, D., Samuel, B.U., Richards, T.A. et al. (2004) Evidence for mitochondrial-derived alternative oxidase in the apicomplexan parasite *Cryptosporidium parvum*: a potential anti-microbial agent target. *International Journal for Parasitology*, 34(3), 297–308. Available from: <https://doi.org/10.1016/j.ijpara.2003.11.002>
- Saha, B., Borovskii, G. & Panda, S.K. (2016) Alternative oxidase and plant stress tolerance. *Plant Signaling & Behavior*, 11(12), e1256530. Available from: <https://doi.org/10.1080/15592324.2016.1256530>
- Schuster, F.L. (2002) Cultivation of pathogenic and opportunistic free-living amebas. *Clinical Microbiology Reviews*, 15(3), 342–354. Available from: <https://doi.org/10.1128/CMR.15.3.342-354.2002>
- Shiba, T., Kido, Y., Sakamoto, K., Inaoka, D.K., Tsuge, C., Tatsumi, R. et al. (2013) Structure of the trypanosome cyanide-insensitive alternative oxidase. *Proceedings of the National Academy of Sciences*, 110(12), 4580–4585. Available from: <https://doi.org/10.1073/pnas.1218386110>
- Sievers, F., Wilm, A., Dineen, D., Gibson, T.J., Karplus, K., Li, W. et al. (2011) Fast, scalable generation of high-quality protein multiple sequence alignments using clustal omega. *Molecular Systems Biology*, 7(1), 539. Available from: <https://doi.org/10.1038/msb.2011.75>
- Stechmann, A., Hamblin, K., Pérez-Brocail, V., Gaston, D., Richmond, G.S.S., van der Giezen, M. et al. (2008) Organelles in *Blastocystis* that blur the distinction between mitochondria and hydrogenosomes. *Current Biology*, 18(8), 580–585. Available from: <https://doi.org/10.1016/j.cub.2008.03.037>
- Tsaousis, A.D., Hamblin, K.A., Elliott, C.R., Young, L., Rosell-Hidalgo, A., Gourlay, C.W. et al. (2018) The human gut colonizer *Blastocystis* respire using complex II and alternative oxidase to buffer transient oxygen fluctuations in the gut. *Frontiers in Cellular and Infection Microbiology*. Available from: <https://doi.org/10.3389/fcimb.2018.00371>
- Tsaousis, A.D., Nývlťová, E., Šuták, R., Hrdý, I. & Tachezy, J. (2014) A nonmitochondrial hydrogen production in *Naegleria gruberi*. *Genome Biology and Evolution*, 6(4), 792–799. Available from: <https://doi.org/10.1093/gbe/evu065>
- Tymł, T., Skulinová, K., Kavan, J., Ditrich, O., Kostka, M. & Dyková, I. (2016) Heterolobosean amoebae from Arctic and Antarctic extremes: 18 novel strains of *Allovalkhampfia*, *Vahlkampfia* and *Naegleria*. *European Journal of Protistology*, 56, 119–133. Available from: <https://doi.org/10.1016/j.ejop.2016.08.003>
- Vanlerberghe, G.C. (2013) Alternative oxidase: a mitochondrial respiratory pathway to maintain metabolic and signaling homeostasis during abiotic and biotic stress in plants. *International Journal of Molecular Sciences*, 14(4), 6805–6847. Available from: <https://doi.org/10.3390/ijms14046805>
- Vassella, E., Probst, M., Schneider, A., Studer, E., Kunz Renggli, C. & Roditi, I. (2004) Expression of a major surface protein of *Trypanosoma brucei* insect forms is controlled by the activity of mitochondrial enzymes. *Molecular Biology of the Cell*. Available from: <https://doi.org/10.1091/mbc.E04-04-0341>
- Waterhouse, A.M., Procter, J.B., Martin, D.M.A., Clamp, M. & Barton, G.J. (2009) Jalview version 2-A multiple sequence alignment editor and analysis workbench. *Bioinformatics*, 25(9),

1189–1191. Available from: <https://doi.org/10.1093/bioinformatics/btp033>

Yan, L., Li, M., Cao, Y., Gao, P., Cao, Y., Wang, Y. et al. (2009) The alternative oxidase of *Candida albicans* causes reduced fluconazole susceptibility. *Journal of Antimicrobial Chemotherapy*, 64(4), 764–773. Available from: <https://doi.org/10.1093/jac/dkp273>

Zaongo, S.D., Shaio, M.-F. & Ji, D.-D. (2018) Effects of culture media on *Naegleria fowleri* growth at different temperatures. *Journal of Parasitology*, 104(5), 451–456. Available from: <https://doi.org/10.1645/18-6>

**How to cite this article:** Cantoni, D., Osborne, A., Taib, N., Thompson, G., Martín-Escolano, R., Kazana, E., et al. (2022) Localization and functional characterization of the alternative oxidase in *Naegleria*. *Journal of Eukaryotic Microbiology*, 69, e12908. <https://doi.org/10.1111/jeu.12908>

## SUPPORTING INFORMATION

Additional supporting information may be found in the online version of the article at the publisher's website.